This article has been accepted for inclusion in a future issue of this journal. Content is final as presented, with the exception of pagination.



# A Physical Model for Metal–Oxide Thin-Film Transistor Under Gate-Bias and Illumination Stress

Jiapeng Li, Lei Lu, Rongsheng Chen, Hoi-Sing Kwok, *Fellow, IEEE*, and Man Wong, *Senior Member, IEEE*

***Abstract*— A negative shift in the turn-on voltage of a metal–oxide thin-film transistor under negative gate-bias and illumination stress has been frequently reported. The stretched-exponential equation, predicated largely on a charge-trapping mechanism, has been commonly used to fit the time dependence of the shift. The fitting parameters, some with unsubstantiated physical origin, are extracted by curve fitting. A more physically based model is presently formulated, incorporating the photogeneration, transport, and trapping of holes. The model parameters of generation energy barrier, hole mobility, and trapping time constant are extracted from the measured gate-bias dependent turn-on voltage shift. It is theoretically deduced and experimentally verified that the degradation kinetics is either generation or transport limited. The model can be further applied to explain the attenuated shift under positive bias and illumination stress, if the screening of the electric field emanating from the gate bias is also accounted for. From the effects of asymmetric source/drain bias applied during stress, it is deduced that the trapping is localized along the length of the channel interface. The turn-on voltage of a transistor after such stress is constrained by the portion of the channel exhibiting the smallest shift.**

***Index Terms*— Asymmetric stress, bias illumination stress, generation or transport limited, indium–gallium–zinc oxide (IGZO), reliability, thin-film transistor (TFT).**

## I. Introduction

WITH their relatively lower process temperature, higher field-effect mobility, lower leakage current, and higher transparency [1], metal–oxide–semiconductors such as zinc oxide and its variants are being pursued as promising alternatives to amorphous silicon for the construction of thin-film transistors (TFTs) in the next-generation flat-panel displays. However, reliability issues of metal–oxide TFTs, particularly those related to gate-bias stress under illumination [2], and their underlying mechanism must be better understood and resolved before the technology is ready for wider industrial adaptation [3].

Among the variants of zinc oxide, indium–gallium–zinc oxide (IGZO) has been most intensely studied. TFTs based on IGZO have been reported to suffer the severest degradation under negative gate-bias and illumination stress (NBIS) [4], as revealed by the dependence of the shift ($\Delta V_{\text{on}}$) of the turn-on voltage ($V_{\text{on}}$) on the stress duration ($t$) [5]. The negative $\Delta V_{\text{on}}$ during NBIS is usually attributed to the trapping of positive charges at or adjacent to the channel/insulator interface [6], [7].

Much has been reported on the analysis of the charge-trapping process by fitting the $t$-dependence of $\Delta V_{\text{on}}$ with a stretched-exponential equation [2], [8], [9] that is parameterized by an extrapolated "saturation" $\Delta V_\infty$ at $t = \infty$, a characteristic trapping time constant $\tau$, and a stretched-exponential factor $\beta$ [10]

$$\Delta V_{\text{on}} = \Delta V_\infty\left[1-e^{-\left(\frac{t}{\tau}\right)^\beta}\right]. \tag{1}$$

However, being a phenomenological fit rather than a physical model, the equation sheds little light on the rich character of the physical processes taking place during stress [4], [10], [11]. Examples of the diverse instability behavior include the different dependence of $\Delta V_{\text{on}}$ on illumination with different wavelengths [11], on the magnitude of the bias, and on positive bias and illumination stress (PBIS) [4]. It is likely such limitation arises from an emphasis only on the charge-trapping dynamics, but ignoring the kinetics of the photogeneration and transport of the responsible charge carriers.

In this paper, IGZO TFTs with thermally induced source/drain (S/D) regions [12] were fabricated to investigate device stability against bias and illumination stress. A simple 1-D "generation-transport-trap" model is proposed for NBIS-induced instability, accounting for the photogeneration and transport of holes across the thickness of the channel, and their eventual trapping at or near the channel/gate-insulator (GI) interface. Model parameters such as energy barrier for generation ($q\phi$), generation rate prefactor ($g_0$), hole mobility ($\mu_{\text{h}}$), and interfacial trapping time constant ($\tau_{\text{s}}$) are extracted from the measured dependence of $\Delta V_{\text{on}}$ on $t$

Manuscript received August 23, 2017; revised October 9, 2017; accepted October 31, 2017. This work was supported by the Partner State Key Laboratory on Advanced Displays and Optoelectronics Technologies under Grant ITC-PSKL12EG02. The review of this paper was arranged by Editor K. Kalna. *(Corresponding author: Jiapeng Li.)*

J. Li and M. Wong are with the Department of Electronic and Computer Engineering, The Hong Kong University of Science and Technology, Hong Kong (e-mail: jliaz@connect.ust.hk; eemwong@ust.hk).

L. Lu and H.-S. Kwok are with the Department of Electronic and Computer Engineering, The Hong Kong University of Science and Technology, Hong Kong, and also with Department of Electronic and Computer Engineering, Jockey Club Institute for Advanced Study, The Hong Kong University of Science and Technology, Hong Kong.

R. Chen is with the Department of Electronic and Computer Engineering, The Hong Kong University of Science and Technology, Hong Kong, and also with the School of Electronic and Information Engineering, South China University of Technology, Guangzhou 510640, China.

Color versions of one or more of the figures in this paper are available online at http://ieeexplore.ieee.org.

Digital Object Identifier 10.1109/TED.2017.2771800

This article has been accepted for inclusion in a future issue of this journal. Content is final as presented, with the exception of pagination.


and the gate bias ($V_g$) during stress. The effects of drain bias ($V_d$) on NBIS-induced instability were also studied. It is deduced that the hole trapping during stress is localized along the length of the channel interface. Consequently, the overall $V_{on}$ of the transfer characteristics after stress is constrained by the portion of the channel suffering the least amount of trapping, thus exhibiting the smallest $\Delta V_{on}$.

## II. Modeling and Experiments

TFT fabrication started with the sputter deposition and patterning of ~80-nm molybdenum (Mo) as the bottom gate electrode on an oxidized silicon wafer. A GI stack consisting of 50-nm silicon nitride topped with 75-nm silicon oxide ($SiO_x$) was deposited in a plasma-enhanced chemical vapor deposition (PECVD) reactor before ~20-nm IGZO was deposited by sputtering from a target with a molar ratio of $In_2O_3$:$Ga_2O_3$:ZnO = 1:1:1. The active island was subsequently patterned and capped with 300-nm gas-permeable $SiO_x$ passivation layer (PL) deposited in the same PECVD apparatus. After the S/D and gate contact holes were opened, gas-impermeable S/D metal electrodes consisting of a stack of sputtered aluminum (Al) on Mo were patterned to partially overlap the gate electrode. The TFT was then "activated" at 400 °C for 4 h in an oxygen atmosphere to thermally induce the formation of the highly conductive S/D regions [13]. Shown in Fig. 1(a)–(c) are, respectively, a schematic of the resulting IGZO TFT, the cross section of the region of the TFT used in numerical simulation, and the coordinate system used to set up the model equations.

The TFTs were subjected to a variety of stress conditions, including pure illumination stress (IS) without bias, negative/positive bias stress (N/PBS) without and with green (~532 nm) or blue (~485 nm) illumination (green-NBIS or blue-N/PBIS). The intensity of the illumination was fixed at 0.4 W/m$^2$, measured using a calibrated photodiode. For both N/PBS and N/PBIS, the $V_g$ during stress was $-20/+20$ V, with the S/D electrodes grounded ($V_s = V_d = 0$ V). The transfer characteristics were measured in the dark after each illumination session using an Agilent 4156C Semiconductor Parameter Analyzer. The delay between the turning off of the light source and the electrical measurement was less than 1 s. $V_{on}$ is defined as the $V_g$ at which an exponential increase in the drain current ($I_d$) is first observed.

It is clear from Fig. 2 that blue-NBIS was the only stress configuration exhibiting a continuous negative shift in $V_{on}$ with $t$. The absence of any significant deterioration of the pseudosubthreshold slope is a strong indication that no new defect states in the bandgap were created during the stress [14]. Because of the invariant transfer characteristics obtained during and after blue-IS and blue-PBIS, and in agreement with the reported fast decay of photocurrent in IGZO [15], long-living excess photogenerated electrons in the channel were eliminated as the cause of the negative $\Delta V_{on}$ [16] for blue-NBIS. Furthermore, the minimally affected $V_{on}$ after PBIS and PBS reflects a good channel/GI interface relatively free of electron trap states.

The negative $\Delta V_{on}$ under blue-NBIS has properly been attributed to the trapping of photogenerated positive charges at or near the interface between the IGZO channel and the $SiO_x$ GI [6], [7], [17], [18]. Both ionized ($V_O^{2+/+}$) oxygen vacancy ($V_O$) defects and holes ($h^+$) have been proposed as possible

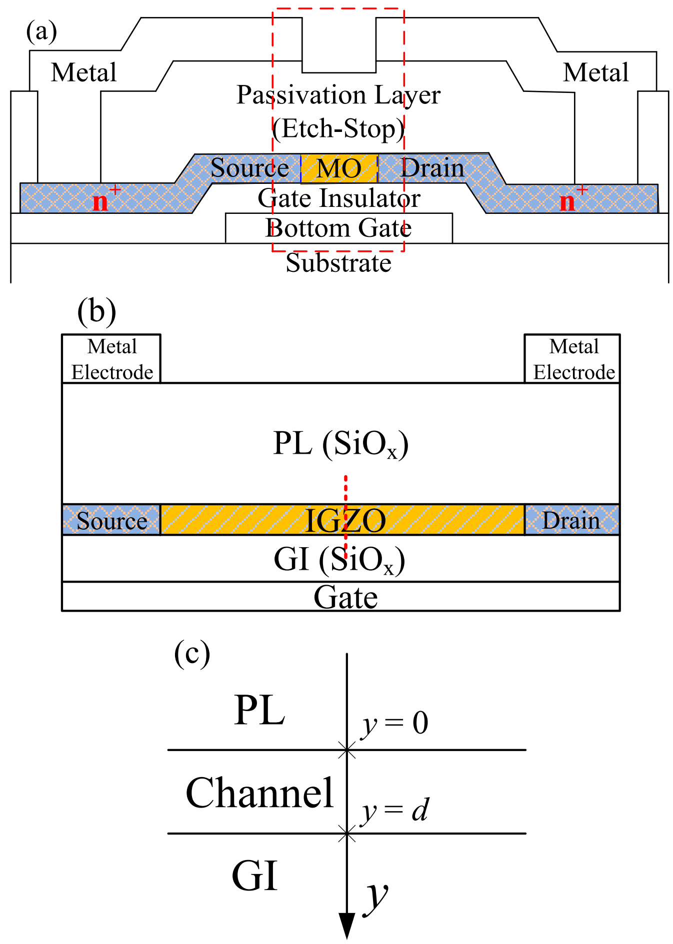


Fig. 1. (a) Schematic of IGZO TFTs with thermally induced and highly conductive S/D regions (cross hatched). (b) Cross section of the portion of a TFT [box bound by dotted line in (a)] under simulation; the electric field along the red line in the middle of the channel is simulated. (c) Coordinate system used to set up the model equations.

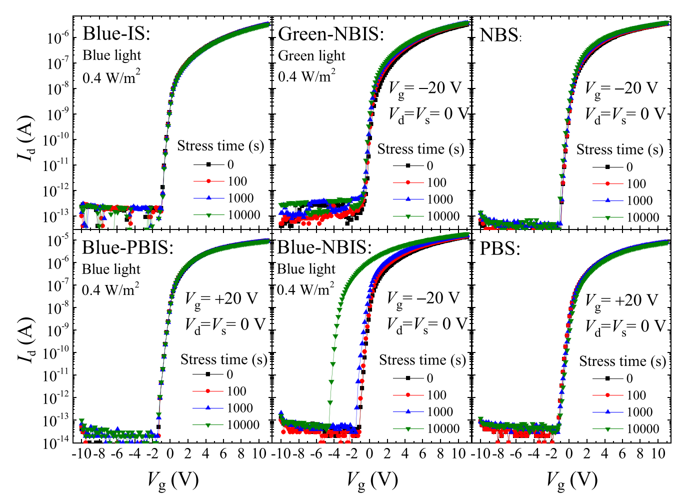


Fig. 2. Time evolution of the transfer characteristics of IGZO TFTs subjected to a variety of stress conditions including IS, N/PBS, and N/PBIS.

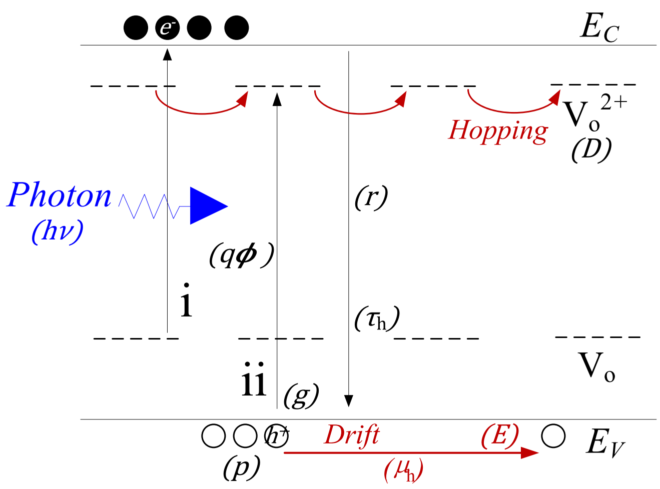


Fig. 3. Energy band diagram describing the photoassisted generation of ionized oxygen vacancies and holes. $E_C$ and $E_V$ are the respective edges of the conduction and valance bands.

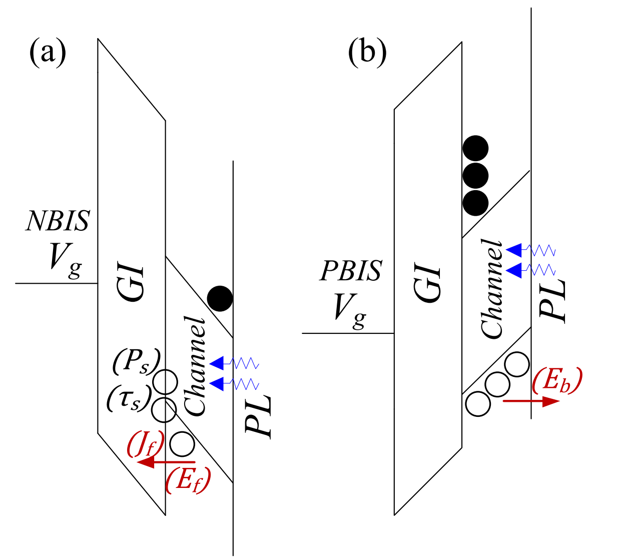


Fig. 4. Schematic of the degradation mechanism in TFTs under (a) NBIS and (b) PBIS.

candidates for such positive charges. Deduced by combining the Einstein relationship with the reported diffusion coefficient and activation energy [19], the room-temperature mobility of an ionized $V_O$ is merely $\sim10^{-27}$ cm$^2$/V $\cdot$ s. This is $\sim$22 orders of magnitude smaller than the theoretically predicted maximum $\mu_h$ of $\sim10^{-5}$ cm$^2$/V$\cdot$s [20]. Consequently, h$^+$ rather than $V_O^{2+/+}$ are the more likely species accounting for the $\Delta V_{on}$ under blue-NBIS.

Holes are photogenerated via a two-step process, as summarized in (2) and (3), and shown schematically in Fig. 3.

1) Photoionization of $V_O$ resulting in the promotion of electrons (e$^-$) to the conduction band and the formation of $V_O^{2+}$. This requires a photon energy of $\sim$2.3 eV [11], [21].
2) h$^+$ generation by the promotion of e$^-$ from the valance band to the $V_O^{2+}$ state. This requires an energy of $\sim$2.8 eV [22], [23]

$$V_O + h\nu \longrightarrow V_O^{2+} + 2e^- \quad (2)$$
$$V_O^{2+} + h\nu \longrightarrow V_O + 2h^+. \quad (3)$$

A model is presently formulated for NBIS-induced $\Delta V_{on}$, based on the following sequence of events: 1) the generation of h$^+$ by photoexcitation; 2) the transport of these h$^+$ across the channel; and 3) the final trapping of the h$^+$ at the interface. It is assumed that the population of photogenerated h$^+$ is small compared to the background of field-induced charge carriers so as not to materially change the electric field ($E$) established in the channel by the $V_g$.

The photogeneration rate $g$ of h$^+$ is given by

$$g = g_0 e^{\frac{-q\phi+h\nu}{k_B T}} \quad (4)$$

where $g_0$ is a constant prefactor related to the density $D$ of $V_O^{2+}$, $q$ is elemental charge, $\phi$ is generation potential barrier, $h$ is Planck's constant, $\nu$ is the frequency of illumination, $k_B$ is Boltzmann's constant, and $T$ is the absolute temperature. Note that under illumination, the effective barrier against generation is reduced by the photon energy ($h\nu$). Consequently, the Boltzmann factor alone contributes to a reduction of $g$ by $\sim10^4$ (originating from a reduction in $h\nu$ by $\sim$0.24 eV) at room temperature when switched from blue to green illumination. The recombination rate $r$ of h$^+$ is expressed by

$$r = \frac{p}{\tau_h} \quad (5)$$

where $p$ is the concentration of h$^+$ due to photogeneration and $\tau_h$ is the corresponding recombination time constant.

Given the much higher electron mobility ($\sim$10 cm$^2$/V $\cdot$ s) than $\mu_h$ in IGZO [13], the photogenerated electrons can be transported rather more quickly than holes across the 20-nm channel thickness ($d$). Therefore, the continuity equation for only the holes needs to be considered during the stress

$$\frac{dp}{dt} = g - r - \frac{1}{q}\frac{dJ}{dy} \approx g_0 e^{\frac{-q\phi+h\nu}{k_B T}} - \frac{p}{\tau_h} - p\mu_h\frac{dE}{dy} = 0 \quad (6)$$

where $J = q\mu_h E p$ is the h$^+$ drift current density and $y$ is defined in Fig. 1(c). Note that $p$ is taken to be the total h$^+$ concentration due to the small intrinsic background concentration of holes in IGZO.

It is reported that $\tau_h \sim 10^{-2}$ s [15], much shorter than the stress duration of 10 000 s. Therefore, the local $p$ is capable of quickly reaching steady state. For IS without bias, steady state $\Rightarrow g = r$ and $J = 0$. One deduces

$$p_0 = g_0 \tau_h e^{\frac{-q\phi+h\nu}{k_B T}} \quad (7)$$

where $p_0$ is the steady-state concentration of h$^+$.

Under the action of $E$ during NBIS, the photogenerated h$^+$ drift to and accumulate at the front interface between IGZO and GI. They are eventually trapped in the interface states. The total amount of trapped holes ($P_s$) is determined by a competition of the drift current density $J_f$ being injected at the front interface and the detrapping process as shown in Fig. 4(a) such that

$$\frac{dP_s}{dt} = \frac{J_f}{q} - \frac{P_s}{\tau_s} \quad (8)$$

where $\tau_s$ is a time constant associated with the interfacial hole traps. It is similar to $\tau$ in (1) but different from $\tau_h$ in (5) for the recombination of the photogenerated electrons and holes in the bulk of the channel. Consequently

$$P_s = \frac{J_f}{q}\tau_s\left(1-e^{-\frac{t}{\tau_s}}\right) = \mu_h E_f p_f \tau_s\left(1-e^{-\frac{t}{\tau_s}}\right) \tag{9}$$

where $E_f$ and $p_f$ are, respectively, the electric field and the $h^+$ concentration at the front interface. A simple nonstretched exponential behavior is thus obtained

$$\Delta V_{on} = \frac{qP_s}{C_{ox}} = \underbrace{\frac{J_f}{C_{ox}}}_{\Delta V_\infty}\tau_s\left(1-e^{-\frac{t}{\tau_s}}\right) \tag{10}$$

where $C_{ox}$ is the effective GI capacitance. Clearly, $J_f$ is the factor determining $\Delta V_\infty$. Two regimes of behavior regarding $\Delta V_{on}$ are discussed in the following.

When the electric field gradient $dE/dy$ is large, such that $r$ in (6) is negligible in comparison, the generated holes at each location across the channel are removed predominately by drift. Consequently, $J_f$ is limited by generation. The $g$-limited $J_{f1}$ is given by

$$J_{f1} = qdg_0 e^{\frac{-q\phi+h\upsilon}{k_B T}}. \tag{11}$$

Thus

$$\Delta V_{on1} = \underbrace{\frac{qdg_0}{C_{ox}}e^{\frac{-q\phi+h\upsilon}{k_B T}}}_{\Delta V_{\infty 1}}\tau_s\left(1-e^{-\frac{t}{\tau_s}}\right) \tag{12}$$

where $\Delta V_{on1}$ is the generation-limited $\Delta V_{on}$ and $\Delta V_{\infty 1}$ is the corresponding saturation value.

For the opposite limiting case of $dE/dy$ being negligible in comparison with $r$, $p$ is dominated by the local equilibrium of generation and recombination, governed by (7). Consequently

$$J_{f2} = q\mu_h E_f p_0. \tag{13}$$

The transport-limited $\Delta V_{on2}$ is given by

$$\Delta V_{on2} = \underbrace{\frac{q\mu_h E_f g_0 \tau_h}{C_{ox}}e^{\frac{-q\phi+h\upsilon}{k_B T}}}_{\Delta V_{\infty 2}}\tau_s\left(1-e^{-\frac{t}{\tau_s}}\right) \tag{14}$$

where $\Delta V_{\infty 2}$ is the corresponding saturation value. Which one of the two mechanisms dominates the $t$-dependence of $\Delta V_{on}$ under NBIS is determined by the relative magnitude of $1/\tau_h$ and $\mu_h dE/dy$ and ultimately the magnitude of $V_g$.

With the S/D electrodes grounded and the blue illumination power density fixed at 0.4 W/m$^2$, the dependence of NBIS induced instability on the magnitude $|V_g|$ between 0 and 30 V was investigated. Two distinct regimes can be observed (Fig. 5) for the dependence of $\Delta V_{on}$ on $V_g$. When $|V_g|$ is lower than 8 V, the $\Delta V_{on}$ after $t = 10\,000$ s depends almost linearly on $V_g$. In this regime, $E$ is relatively small, thus it is the limiting factor in regulating $J_f$. For $|V_g|$ greater than 8 V, a relatively constant $\Delta V_{on}$ was obtained, despite almost quadrupling $|V_g|$ from 8 to 30 V. This is the regime in which $P_s$ is limited by the generation of holes.

$\Delta V_{on}$ extracted in the $g$-limited regime at $V_g = -30$ V is plotted in Fig. 6. For $t < 3000$ s, the roughly linear

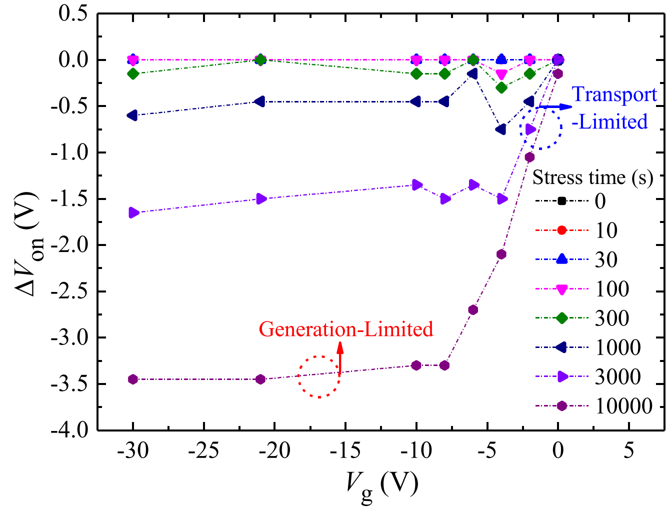


Fig. 5. Dependence of $\Delta V_{on}$ on $V_g$ for IGZO TFTs subjected to NBIS for different $t$.

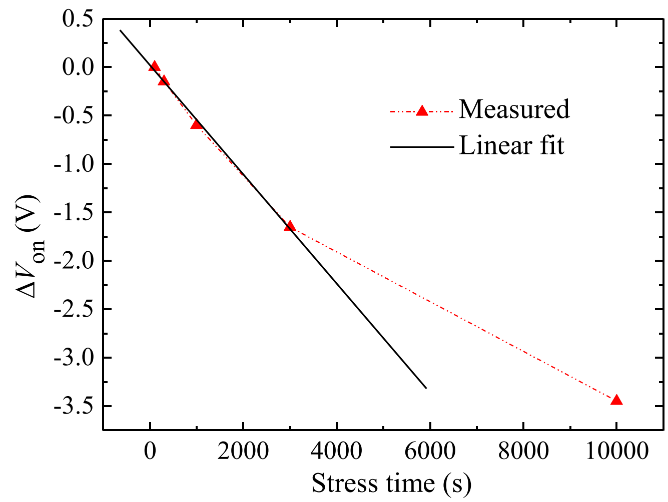


Fig. 6. Time evolution of $\Delta V_{on}$ during NBIS at $V_g = -30$ V.

dependence of $\Delta V_{on}$ on $t$ reflects the fact that the interface traps are far from being saturated with captured holes; hence, the corresponding saturation in Fig. 5 is a consequence of the limitation by $h^+$ generation in the bulk of the channel. For $t > 3000$ s, the time rate of shift reduces as more of the trap states are filled, leading to a gradual saturation of $\Delta V_{on}$ when $t$ continues to increase.

NBIS at elevated temperature ($T$) up to $T = 80$ °C was investigated, with $V_g$ fixed at $-21$ V and using the same illumination condition. This is also commonly known as the negative bias temperature and illumination stress (NBTIS). Shown in Fig. 7 is the $t$-dependence of the resulting $\Delta V_{on}$. Included also are the analytical fits using the common stretched-exponential form according to (1) and the $g$-limited simple exponential form according to (12). Both fits are reasonable, with the corresponding average $\tau_s$ fluctuating around ~6000 and ~7500 s (inset of Fig. 7), thus indicating a relatively long-trapping time constant.

$\tau_s$ extracted at different $T$ is shown in Fig. 8(a), lacking a clear dependence on $T$. The corresponding relative fluctuation

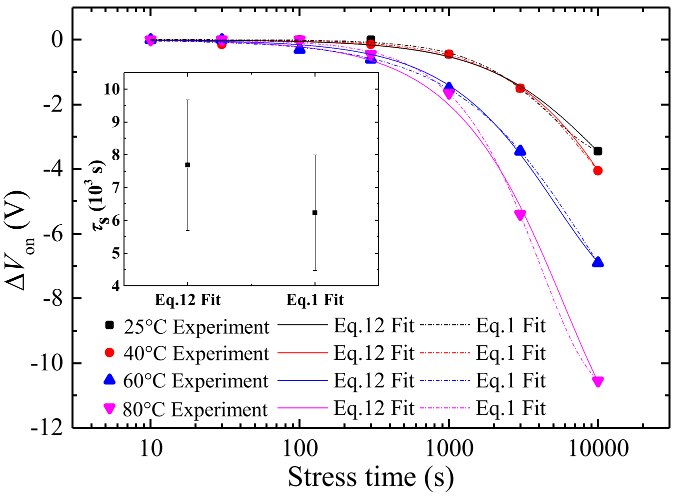


Fig. 7. $t$-dependence of $\Delta V_{\text{on}}$ after NBTIS at $V_g = -21$ V, and analytical fits using the generation–transport–trap model (12) and stretched-exponential equation (1). Inset: extracted $\tau_s$ for both fits.

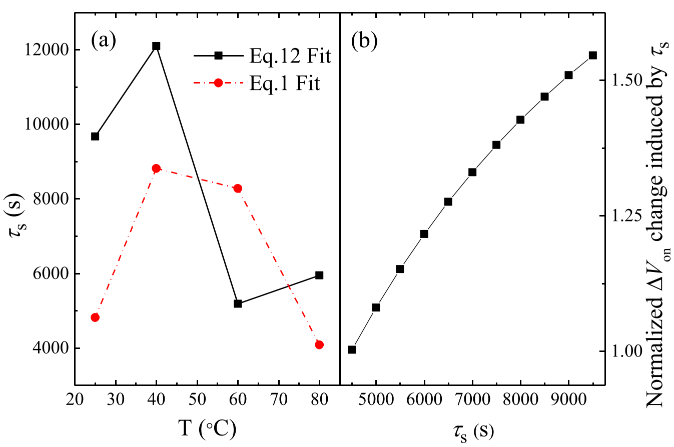


Fig. 8. (a) Variation of extracted $\tau_s$ with $T$. (b) Normalized $\Delta V_{\text{on}}$ change induced by the variation of extracted $\tau_s$.

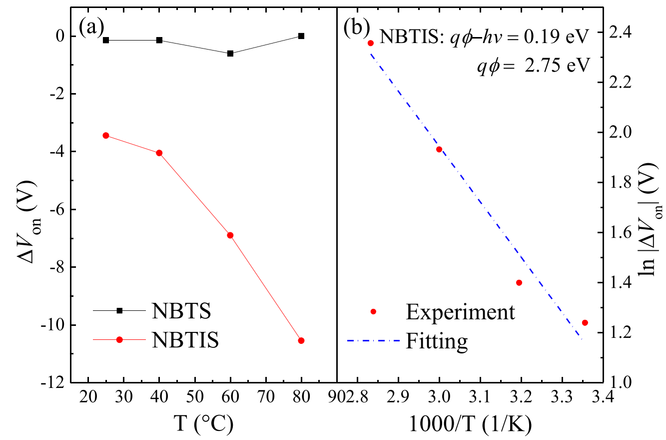


Fig. 9. (a) Dependence of $\Delta V_{\text{on}}$ on $T$ for IGZO TFTs subjected to NBTS and NBTIS. (b) $\ln|\Delta V_{\text{on}}|$ as a function of $1000/T$.

TABLE I
EXTRACTED PARAMETERS OF GENERATION–TRANSPORT–TRAP MODEL BASED ON MEASURED RELIABILITY PERFORMANCE OF FABRICATED IGZO TFTS

| Parameters | Unit | Value |
|---|---|---|
| Generation energy barrier $q\phi$ | eV | ~2.75 |
| Trap time constant $\tau_s$ | s | ~7500 |
| Holes mobility $\mu_h$ | $cm^2/Vs$ | $\sim 10^{-9}$ |
| Generation rate pre-factor $g_0$ | $/cm^3 s$ | $\sim 10^{17}$ |
| Generation rate $g$ | $/cm^3 s$ | $\sim 10^{14}$ |
| Steady-state hole concentration $p_0$ | $/cm^3$ | $\sim 10^{12}$ |

of $\tau_s(1 - e^{-(t/\tau_s)})$, thus its contribution to $\Delta V_{\text{on}}$ variation according to (12), is shown in Fig. 8(b). The variation of about $\sim$50% for $\tau_s$ ranging from 5000 to 9000 s is small compared to the 400% increase of $\Delta V_{\text{on}}$ when $T$ was increased from 25 °C to 80 °C. The larger variation should properly be assigned to the $e^{(-q\phi+h\nu/k_B T)}$ exponential term in $\Delta V_{\infty 1}$. Consequently, the average $\tau_s$ of 7500 s is used for the extraction of the model parameters.

Shown in Fig. 9(a) is the $T$-dependence of $\Delta V_{\text{on}}$ after 10 000-s NBTIS in linear scale and in Fig. 9(b) is the same in Arrhenius plot. Higher temperature obviously enhances the generation rate of holes [24]. From the slope of the plot in Fig. 9(b), an energy barrier $q\phi$ of 2.75 eV is obtained. This is close to the reported energy difference of $\sim$2.8 eV [22], [23] between the valence band edge and the $V_O^{2+}$ level. Because of the large $q\phi$ compared with the thermal energy ($\sim$31 meV) even at 80 °C, it is small wonder that $\Delta V_{\text{on}}$ is negligible under NBTS, as shown at the top of Fig. 8(a).

Since $V_{\text{on}} \sim 0$ V, $E_f$ can be approximated by assuming the entire $V_g$ is dropped across the thickness ($d_{\text{ox}}$) of the GI due to interfacial band pinning in IGZO, i.e

$$E_f \approx \frac{V_g}{d_{\text{ox}}} \frac{\varepsilon_{\text{ox}}}{\varepsilon_{\text{IGZO}}} \tag{15}$$

where $\varepsilon_{\text{ox}}$ and $\varepsilon_{\text{IGZO}}$ are the respective effective dielectric constants of the GI and IGZO. The same extraction procedure is next applied to the set of $\Delta V_{\text{on}}$ obtained in the transport-limited regime shown in Fig. 5, this time using (14). The extracted model parameters are summarized in Table I.

The different behavior of N/PBIS was studied by estimating the distribution of $E$ across $d$ (Fig. 10) using a commercial device simulator and the schematic device cross section shown in Fig. 1(b). The highly conductive S/D regions, with a low resistivity of $\sim 10^{-2}$ $\Omega \cdot$ cm [4], were treated as conductors. Other physical parameters and dimensions were unchanged.

Because of the change in the direction of $E$, photogenerated holes are transported to the IGZO/PL back interface during PBIS. It is clear that $|E_b|$, the magnitude of the electric field at the back interface during PBIS is significantly attenuated (by $\sim$500 times at $|V_g| = 20$ V) compared to $|E_f|$,

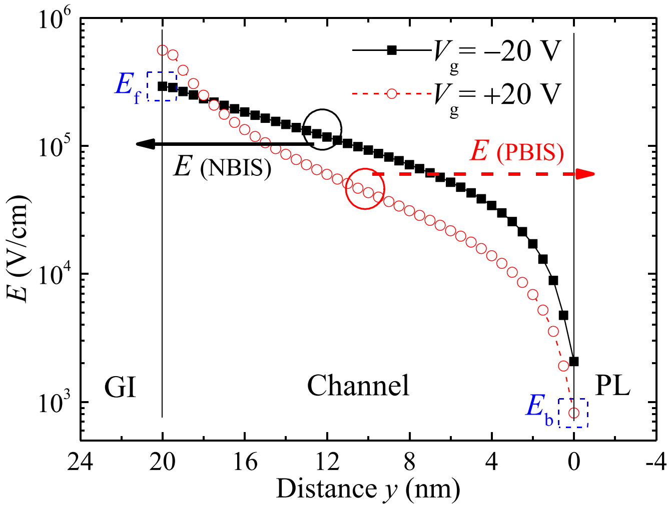


Fig. 10. Simulated distribution of $E$ across the channel at $V_g = \pm 20$ V. $E_f/E_b$ is responsible for the transport of holes near the corresponding interfaces under N/PBIS, respectively.

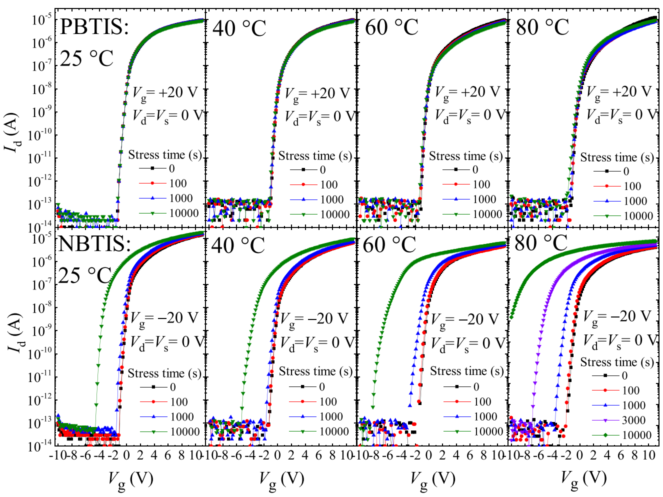


Fig. 11. Comparison of the time evolution of the transfer curves of TFTs subjected to P/NBTIS.

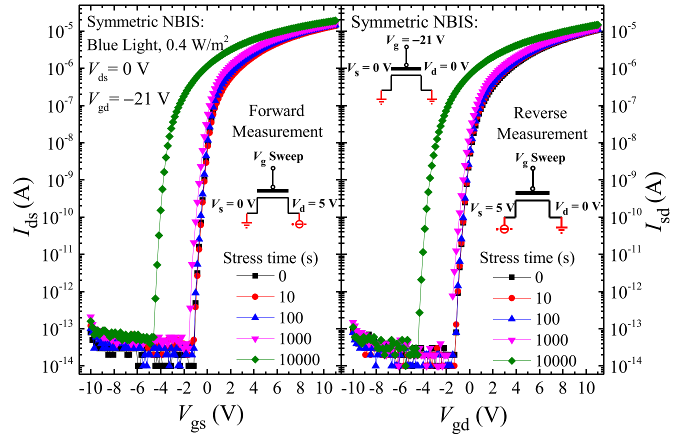


Fig. 12. Time evolution of the forward (Left: $I_{ds}$ versus $V_{gs}$ at $V_{ds} = 5$ V) and reverse (Right: $I_{sd}$ versus $V_{gd}$ at $V_{sd} = 5$ V) transfer curves subjected to NBIS with symmetric S/D bias.

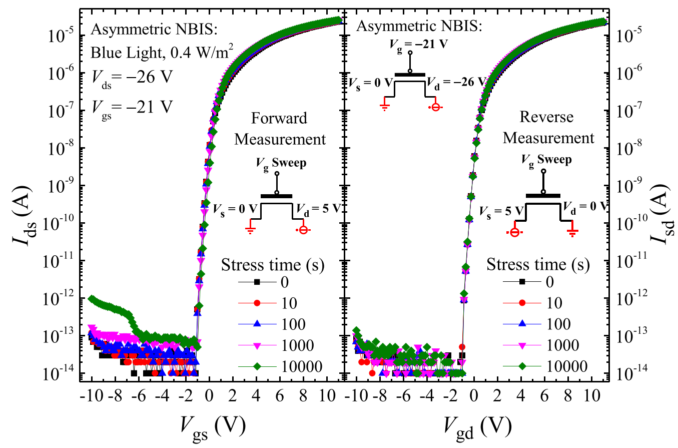


Fig. 13. Time evolution of the forward (Left: $I_{ds}$ versus $V_{gs}$ at $V_{ds} = 5$ V) and reverse (Right: $I_{sd}$ versus $V_{gd}$ at $V_{sd} = 5$ V) transfer curves subjected to NBIS with asymmetric S/D bias.

the magnitude of the electric field at the front interface during NBIS. The weak $E_b$ leads to a slow migration, hence collection, of holes, thus a significant attenuation in the PBIS (Fig. 2)- and PBTIS-induced (Fig. 11) $\Delta V_{on}$ over $t$. The different band-bending configurations during N/PBIS have been schematically shown in Fig. 4. The simulated $|E_f| \sim 3 \times 10^5$ V/cm is close to the theoretical approximate of $5.8 \times 10^5$ V/cm given in (15).

## III. Effects of Asymmetric S/D Bias

The forward and reverse families of transfer characteristics upon reversal of the S/D bias of an IGZO TFT subjected to NBIS with symmetrically grounded S/D regions are shown in Fig. 12. As expected, the two families are similar, with $\Delta V_{on}$ showing indistinguishable $t$-dependence.

It is clear from the schematic device cross section shown in Fig. 1(a) that $E$ is generally nonuniform across the length of the channel between the S/D regions. In fact, $|E|$ would be the smallest in the middle of the channel if both the S/D electrodes were grounded during NBIS. It can be deduced from (14) that $\Delta V_{on}$ reduces with decreasing $|E|$. Since $\Delta V_{on} < 0$ V, the turning on of a stressed TFT is thus controlled by the portion along the channel with the smallest $|\Delta V_{on}|$. In the case of a TFT subjected to symmetric NBIS with grounded S/D electrodes, the point of minimum stress is located in the middle of the channel.

The point of the minimum stress can be displaced from the middle of the channel by breaking the symmetry of grounded S/D during stress. With a grounded source $V_s = 0$ V but a $V_d = -26$ V during NBIS, the resulting forward and reverse families of characteristics are shown in Fig. 13. The two are still more or less identical, except $\Delta V_{on} \approx 0$ V. Since $V_g$ was more positive than $V_d$ during such stress, the drain end was actually subjected to PBIS. Consequently, it is this end that controls the turning on of the stressed TFT, hence the small $|\Delta V_{on}|$ of $\sim 0$ V. This behavior can be nicely captured using a circuit of serially connected TFTs shown in the inset of Fig. 14, with the limiting TFT near the drain end exhibiting a smaller $\Delta V_{on}$.

Clearly, NBIS can be performed by setting $V_d$ [5], [25] over a range that changes the stress condition at the drain end

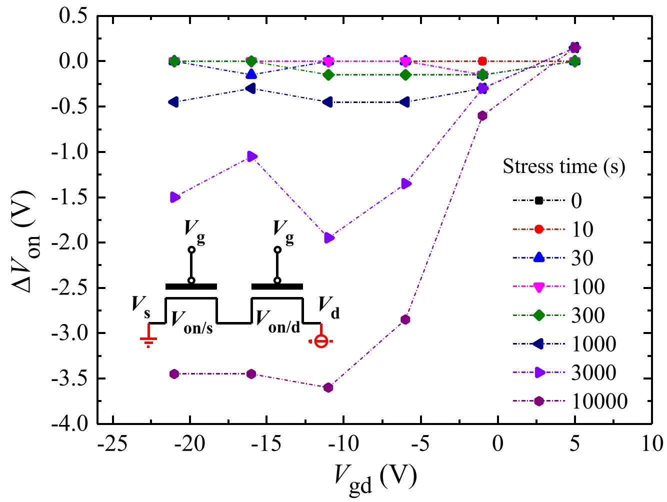


Fig. 14. Dependence of $\Delta V_{on}$ of TFTs under NBIS on the potential difference $V_{gd}$ from gate to drain. Inset: circuit schematic of serially connected TFTs near the source and drain ends of the channel.

continuously from NBIS to PBIS. Such a detailed study has indeed been carried out, and the results are shown in Fig. 14, with $V_g$ and $V_s$ fixed, respectively, at $-21$ and 0 V, but $V_d$ changed from 0 to $-26$ V.

It can be seen that for a given $t$, $|\Delta V_{on}|$ increases continuously as $V_{gd} \equiv V_g - V_d$ decreases from 5 to $-35$ V and saturates beyond $V_{gd} \approx -10$ V. This is consistent with the two regimes of degradation kinetics reported in Fig. 5.

## IV. Conclusion

The stretched-exponential equation, predicated largely on a charge-trapping mechanism, has been commonly used to fit the time dependence of the shift in the turn-on voltage of a metal–oxide TFT under NBIS. Constrained by its emphasis on only the charge-trapping dynamics, the model cannot be used to fully account for the rich character of the physical processes taking place during the stress. A more physically based model is presently formulated, incorporating the photogeneration, transport, and trapping of holes. For indium–gallium–zinc oxide, the respective model parameters of generation energy barrier ~2.75 eV, hole mobility $\sim 10^{-9}$ cm$^2$/V $\cdot$ s, and trapping time constant ~7500 s are extracted from the measured gate-bias dependent turn-on voltage shift. It is theoretically deduced and experimentally verified that the degradation kinetics is either generation or transport limited, depending on the magnitude and direction of the local electric field inside the channel but normal to the channel/interface during the stress. The model can be further applied to explain the attenuated shift under PBIS, when the screening of the electric field emanating from the gate bias has been accounted for. From the effects of asymmetric S/D bias applied during a bias illumination stress, it is deduced that hole trapping is localized along the length of the channel interface. The turn-on voltage of a transistor after such stress is constrained by the portion of the channel exhibiting the smallest shift. Since the model is developed to describe an intrinsic degradation mechanism within the IGZO active layer, it is believed that the proposed generation-transport-trap model is equally suitable for describing similar degradation in other structures built around similar active layers—if the structure induced variation in the distribution of electric field is accounted for.

## Acknowledgment

The authors would like to thank the Nanosystem Fabrication Facility, The Hong Kong University of Science and Technology, Hong Kong, for device fabrication.

## References

[1] E. Fortunato, P. Barquinha, and R. Martins, "Oxide semiconductor thin-film transistors: A review of recent advances," *Adv. Mater.*, vol. 24, no. 22, pp. 2945–2986, Jun. 2012, doi: 10.1002/adma.201103228.

[2] T.-Y. Hsieh, T.-C. Chang, T.-C. Chen, and M.-Y. Tsai, "Review of present reliability challenges in amorphous In-Ga-Zn-O thin film transistors," *ECS J. Solid State Sci. Technol.*, vol. 3, no. 9, pp. Q3058–Q3070, Aug. 2014, doi: 10.1149/2.013409jss.

[3] J. K. Jeong, "The status and perspectives of metal oxide thin-film transistors for active matrix flexible displays," *Semicond. Sci. Technol.*, vol. 26, no. 3, p. 034008, Feb. 2011, doi: 10.1088/0268-1242/26/3/034008.

[4] J. Li, L. Lu, Z. Feng, H. S. Kwok, and M. Wong, "An oxidation-last annealing for enhancing the reliability of indium-gallium-zinc oxide thin-film transistors," *Appl. Phys. Lett.*, vol. 110, no. 14, p. 142102, Apr. 2017, doi: http://dx.doi.org/10.1063/1.4979649.

[5] D. Wang, M. P. Hung, J. Jiang, T. Toda, and M. Furuta, "Suppression of degradation induced by negative gate bias and illumination stress in amorphous InGaZnO thin-film transistors by applying negative drain bias," *ACS Appl. Mater. Interfaces*, vol. 6, no. 8, pp. 5713–5718, Apr. 2014, doi: 10.1021/am500300g.

[6] K. H. Ji *et al.*, "Effect of high-pressure oxygen annealing on negative bias illumination stress-induced instability of InGaZnO thin film transistors," *Appl. Phys. Lett.*, vol. 98, no. 10, pp. 1–4, Mar. 2011, doi: http://dx.doi.org/10.1063/1.3564882.

[7] S. Hong, S. Lee, M. Mativenga, and J. Jang, "Reduction of negative bias and light instability of a-IGZO TFTs by dual-gate driving," *IEEE Electron Device Lett.*, vol. 35, no. 1, pp. 93–95, Jan. 2014, doi: 10.1109/LED.2013.2290740.

[8] T.-C. Chen *et al.*, "Investigating the degradation behavior caused by charge trapping effect under DC and AC gate-bias stress for InGaZnO thin film transistor," *Appl. Phys. Lett.*, vol. 99, no. 2, pp. 97–100, Jul. 2011, doi: http://dx.doi.org/10.1063/1.3609873.

[9] M. P. Hung, D. Wang, T. Toda, J. Jiang, and M. Furuta, "Quantitative analysis of hole-trapping and defect-creation in InGaZnO thin-film transistor under negative-bias and illumination-stress," *ECS J. Solid State Sci. Technol.*, vol. 3, no. 9, pp. Q3023–Q3026, Jul. 2014, doi: 10.1149/2.005409jss.

[10] J.-M. Lee, I.-T. Cho, J.-H. Lee, and H.-I. Kwon, "Bias-stress-induced stretched-exponential time dependence of threshold voltage shift in InGaZnO thin film transistors," *Appl. Phys. Lett.*, vol. 93, no. 9, pp. 093504-1–093504-3, 2008, doi: http://dx.doi.org/10.1063/1.2977865.

[11] X. Huang *et al.*, "Electrical instability of amorphous indium-gallium-zinc oxide thin film transistors under monochromatic light illumination," *Appl. Phys. Lett.*, vol. 100, no. 24, pp. 243505-1–243505-4, Jun. 2012, doi: 10.1063/1.4729478.

[12] L. Lu and M. Wong, "A bottom-gate indium-gallium-zinc oxide thin-film transistor with an inherent etch-stop and annealing-induced source and drain regions," *IEEE Trans. Electron Devices*, vol. 62, no. 2, pp. 574–579, Feb. 2015, doi: 10.1109/TED.2014.2375194.

[13] L. Lu, J. Li, Z. Q. Feng, H.-S. Kwok, and M. Wong, "Elevated-metal–metal-oxide thin-film transistor: Technology and characteristics," *IEEE Electron Device Lett.*, vol. 37, no. 6, pp. 728–730, Apr. 2016, doi: 10.1109/LED.2016.2552638.

[14] M. P. Hung, D. Wang, J. Jiang, and M. Furuta, "Negative bias and illumination stress induced electron trapping at back-channel interface of InGaZnO thin-film transistor," *ECS Solid State Lett.*, vol. 3, no. 3, pp. Q13–Q16, Jan. 2014, doi: 10.1149/2.010403ssl.

[15] H.-W. Liu, P.-C. Chan, J.-H. Lin, C.-Y. Chang, and Y.-H. Tai, "Analysis of the short-term response in the drain current of a-IGZO TFT to light pulses," *IEEE Electron Device Lett.*, vol. 38, no. 7, pp. 887–889, Jul. 2017, doi: 10.1109/LED.2017.2705701.

[16] E. Lee, M. D. H. Chowdhury, M. S. Park, and J. Jang, "Effect of top gate bias on photocurrent and negative bias illumination stress instability in dual gate amorphous indium-gallium-zinc oxide thin-film transistor," *Appl. Phys. Lett.*, vol. 107, no. 23, p. 233509, Dec. 2015, doi: http://dx.doi.org/10.1063/1.4937441.
[17] Y. J. Kim *et al.*, "Photobias instability of high performance solution processed amorphous zinc tin oxide transistors," *ACS Appl. Mater. Interfaces*, vol. 5, no. 8, pp. 3255–3261, Apr. 2013, doi: 10.1021/am400110y.
[18] J. G. Um, M. Mativenga, and J. Jang, "Mechanism of positive bias stress-assisted recovery in amorphous-indium-gallium-zinc-oxide thin-film transistors from negative bias under illumination stress," *Appl. Phys. Lett.*, vol. 103, no. 3, p. 033501, Jul. 2013, doi: http://dx.doi.org/10.1063/1.4813747.
[19] K. Watanabe *et al.*, "Surface reactivity and oxygen migration in amorphous indium-gallium-zinc oxide films annealed in humid atmosphere," *Appl. Phys. Lett.*, vol. 103, no. 20, p. 201904, Nov. 2013, doi: http://dx.doi.org/10.1063/1.4829996.
[20] K. A. Stewart, B.-S. Yeh, and J. F. Wager, "Amorphous semiconductor mobility limits," *J. Non-Cryst. Solids*, vol. 432, pp. 196–199, Jan. 2016, doi: 10.1016/j.jnoncrysol.2015.10.005.
[21] J. Bang, S. Matsuishi, and H. Hosono, "Hydrogen anion and subgap states in amorphous In-Ga-Zn-O thin films for TFT applications," *Appl. Phys. Lett.*, vol. 110, no. 23, p. 232105, Jun. 2017. [Online]. Available: http://dx.doi.org/10.1063/1.4985627.
[22] P. Migliorato, M. D. H. Chowdhury, J. G. Um, M. Seok, and J. Jang, "Light/negative bias stress instabilities in indium gallium zinc oxide thin film transistors explained by creation of a double donor," *Appl. Phys. Lett.*, vol. 101, no. 12, p. 123502, 2012, doi: http://dx.doi.org/10.1063/1.4752238.
[23] S. Lee, A. Nathan, S. Jeon, and J. Robertson, "Oxygen defect-induced metastability in oxide semiconductors probed by gate pulse spectroscopy," *Scientific reports*, vol. 5, Oct. 2015, Art. no. 14902, doi: 10.1038/srep14902.
[24] T. Chen, Y. Kuo, T.-C. Chang, M.-C. Chen, and H.-M. Chen, "Mechanism of *a*-IGZO TFT device deterioration—Llumination light wavelength and substrate temperature effects," *J. Phys. D, Appl. Phys.*, vol. 50, no. 42, p. 42LT02, Aug. 2017.
[25] S.-B. Seo *et al.*, "Drain bias effect on the instability of amorphous indium gallium zinc oxide thin film transistor," *Thin Solid Films*, vol. 547, pp. 263–266, Nov. 2013, doi: 10.1016/j.tsf.2012.12.109.

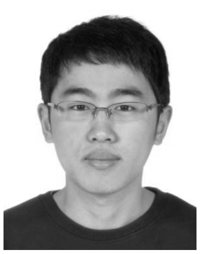

**Jiapeng Li** received the B.S. degree in physics from Peking University, Beijing, China, in 2013. He is currently pursuing the Ph.D. degree with the Department of Electronic and Computer Engineering, The Hong Kong University of Science and Technology, Kowloon, Hong Kong.

His research focuses on the characterization and passivation of thin film transistors based on metal oxide materials, especially Zinc Oxide and its variant Indium Gallium Zinc Oxide.

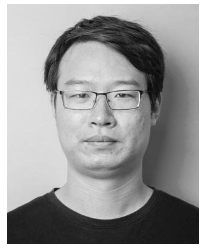

**Lei Lu** received the Ph.D. degree in electrical engineering from Department of Electronic and Computer Engineering, The Hong Kong University of Science and Technology, Hong Kong, in 2014.

His current research interests include the annealing behaviors of ZnO-based metal oxide materials, and the fabrication and reliability study of TFTs based on metal oxides and their applications to touch-panel systems.

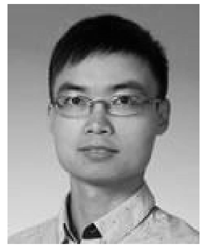

**Rongsheng Chen** received the Ph.D. degree from the Department of Electronic and Computer Engineering, The Hong Kong University of Science and Technology, Hong Kong, in 2013.

His current research interests include novel compound thin-film transistors based on ZnO, IGZO, and GaN, and their application in active matrix displays.

**Hoi-Sing Kwok** (M'78–SM'84–F'05) received the Ph.D. degree in applied physics from Harvard University, Cambridge, MA, USA, in 1978.

He joined The Hong Kong University of Science and Technology, Hong Kong, in 1992, where he is currently the Director of the Center for Display Research and the State Key Laboratory on Advanced Displays and Optoelectronics Technologies.

**Man Wong** (S'83–M'88–SM'00) received the Ph.D. degree in electrical engineering from Stanford University, Stanford, CA, USA, in 1988.

He is currently with the Department of Electronic and Computer Engineering, The Hong Kong University of Science and Technology, Hong Kong. His research interests include micro-fabrication technology, device structure and material, physics and technology of thin-film transistor, organic light-emitting diode display technology, modeling and implementation of integrated micro-systems.